Hyperfine Interactions (2020) 241:27
https://doi.org/10.1007/s10751-020-1701-9

Effect of iron oxide nanoparticles functionalization by citrate analyzed using Mössbauer spectroscopy

Michael V. Ushakov[1] · **M. H. Sousa**[2] · **Paulo C. Morais**[3,4] · **Ernő Kuzmann**[5] · **Vladimir A. Semionkin**[1] · **Michael I. Oshtrakh**[1]

Abstract

Comparison of the Mössbauer spectra of the as-prepared native iron oxide nanoparticles (IONs) and the citrate-functionalized IONs demonstrates differences in the spectral shapes at room temperature and variations of the ^{57}Fe hyperfine parameters at 80 K. The observed differences are claimed to result from capping the IONs with citrate, thus decreasing the particle-particle interaction while promoting interaction of the outer atomic layers of the IONs with the surface molecular coating.

Keywords Mössbauer spectroscopy · Iron oxide nanoparticles · Surface functionalization · Hyperfine parameters

---

This article is part of the Topical Collection on *Proceedings of the International Conference on the Applications of the Mössbauer Effect (ICAME2019), 1-6 September 2019, Dalian, China*
Edited by Tao Zhang, Junhu Wang and Xiaodong Wang

✉ Michael I. Oshtrakh
oshtrakh@gmail.com

Michael V. Ushakov
um.mjolnir@gmail.com

M. H. Sousa
mhsousa@unb.br

Paulo C. Morais
pcmor@unb.br

Ernő Kuzmann
kuzmann@caesar.elte.hu

Vladimir A. Semionkin
sva1946@mail.ru

Extended author information available on the last page of the article

1 Introduction

Iron oxide nanoparticles (IONs) are developed for elaborating magnetic fluids for a long time [1–3]. There are numerous studies by various techniques, including Mössbauer spectroscopy, on the effect of different IONs' preparations, size distribution, shape modulation, surface functionalization, encapsulating, etc. Functionalization is important for further modification of IONs' surface to address various features in biomedical applications (see [3–5]). Surface coating leads to interaction of coating molecules with the IONs surface that can change the magnetic properties of the latter (see, for instance, [6–10]). Recently, it has been shown that magnetic nanoparticles presenting average sizes between 10 and 14 nm and functionalized with different carboxylic acids are superparamagnetic at 80 K [11, 12]. In the present study, the effect of maghemite nanoparticles (NPs) functionalization with citrate is analyzed using Mössbauer spectroscopy.

2 Experimental

As schematically shown in Fig. 1, citrate-functionalized maghemite (γ-Fe_2O_3) NPs were synthesized using a slightly modified procedure already described in [5]. Briefly, 50 mL of aqueous solution containing 50 mmol of Fe^{2+}, 25 mmol of Fe^{3+} and 20 mmol of HCl were quickly poured into 250 mL of NH_4OH aqueous solution (1 mol/L), under vigorous stirring (1000 rpm) at room temperature. The as-formed black precipitate of magnetite (Fe_3O_4) was magnetically separated and washed several times with water until the solution reached neutral pH. Then, the precipitate was acidified with HNO_3 aqueous solution (0.5 mol/L) and magnetically separated from the supernatant. Next, the slurry containing magnetite was oxidized to maghemite by boiling with 0.5 mol/L $Fe(NO_3)_3$ for 30 min. The as-treated precipitate (essentially maghemite) was removed out from the solution by magnetic decantation and labeled as sample FM.

Maghemite NPs functionalized with citrate were prepared from the as-produced bare maghemite (sample FM) using trisodium citrate solution (1.0 mol/L) at 80 °C for 30 min (molar ratio of citrate to iron = 0.1). The obtained precipitate was magnetically collected, washed twice with acetone (excess of acetone evaporated), and labeled as sample FMC.

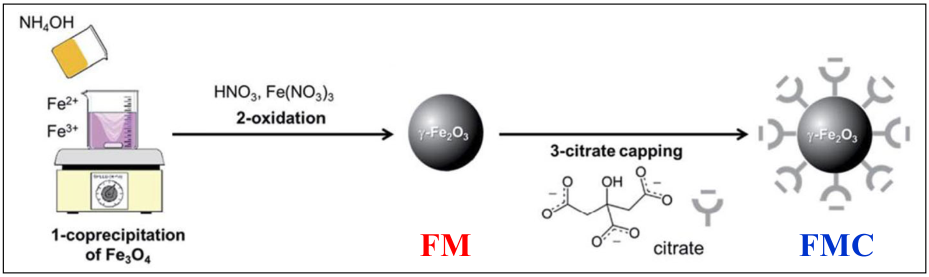

Fig. 1 Scheme of maghemite nanoparticles preparation: **FM** – as-prepared sample, **FMC** – nanoparticles functionalized with citrate (adopted from [5])

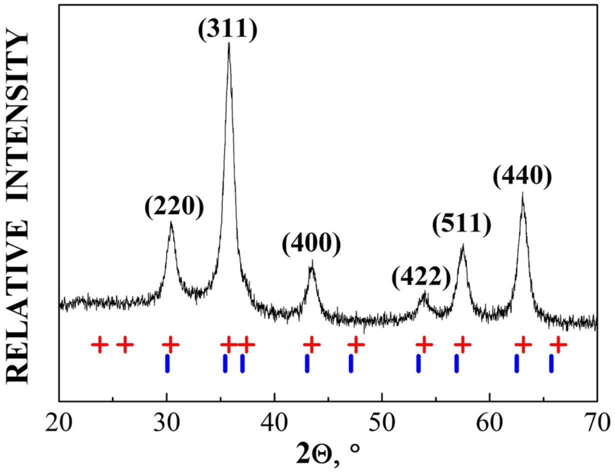

Fig. 2 X-ray diffraction pattern of the as-prepared FM sample. Symbols "+" and "|" indicate peak positions for maghemite (JCPDS 39–1346) and magnetite (JCPDS 19–0629), respectively

Powdered samples for Mössbauer spectroscopy were prepared with surface thickness of 8–10 mg Fe/cm^2.

The FM sample was characterized using X-ray diffraction (XRD). Powder analysis of the sample was carried out with a Miniflex 600 diffractometer (Rigaku) over 2Θ range of 20–70° using Cu-K$_\alpha$ radiation ($\lambda = 1.541$ Å) and operating at 40 kV and 30 mA. Size and morphology of the as-produced FM sample were examined by transmission and high-resolution transmission electron microscopy (TEM and HRTEM) using a JEOL 1100 apparatus.

The room temperature Mössbauer spectra of the FM and FMC samples were measured using an automated precision Mössbauer spectrometric system, built on the base of the SM-2201 spectrometer, with a saw-tooth shape velocity reference signal formed by the digital-analog converter using discretization of 2^{12} (quantification of the velocity reference signal using 4096 steps). Details and characteristics of this spectrometer and the system as well as this method's features were described in [13, 14]. The 1.0×10^9 Bq ^{57}Co in rhodium matrix (Ritverc GmbH, St. Petersburg) is kept at room temperature. The Mössbauer spectra were measured in transmission geometry with moving absorber and recorded in 4096 channels. The 80 K Mössbauer spectra of the FM and FMC samples were measured using a conventional Wissel spectrometer with the triangular velocity reference signal formed using quantification with 512 steps (low velocity resolution) and liquid nitrogen cryostat. The ~1.8×10^9 Bq ^{57}Co in rhodium matrix source (Ritverc GmbH, Saint-Petersburg) is kept at room temperature.

The 80 K Mössbauer spectra were computer fitted by the least squares procedure with MossWinn code [15] after folding using a Lorentzian line shape in different ways. Firstly, the Mössbauer spectra were fitted by the hyperfine field distribution with further fitting the distribution function. Then, the Mössbauer spectra were fitted by the independent magnetic sextets. The spectral parameters such as: isomer shift, δ, quadrupole shift for magnetically split components, ε, magnetic hyperfine field, B, line width, Γ, relative subspectrum area, A, and normalized statistical quality of the fit, χ^2, were determined. Criteria of the best fit were differential spectrum, the value of χ^2, and physical meaning of parameters. Values of δ are given relative to α-Fe at 295 K.

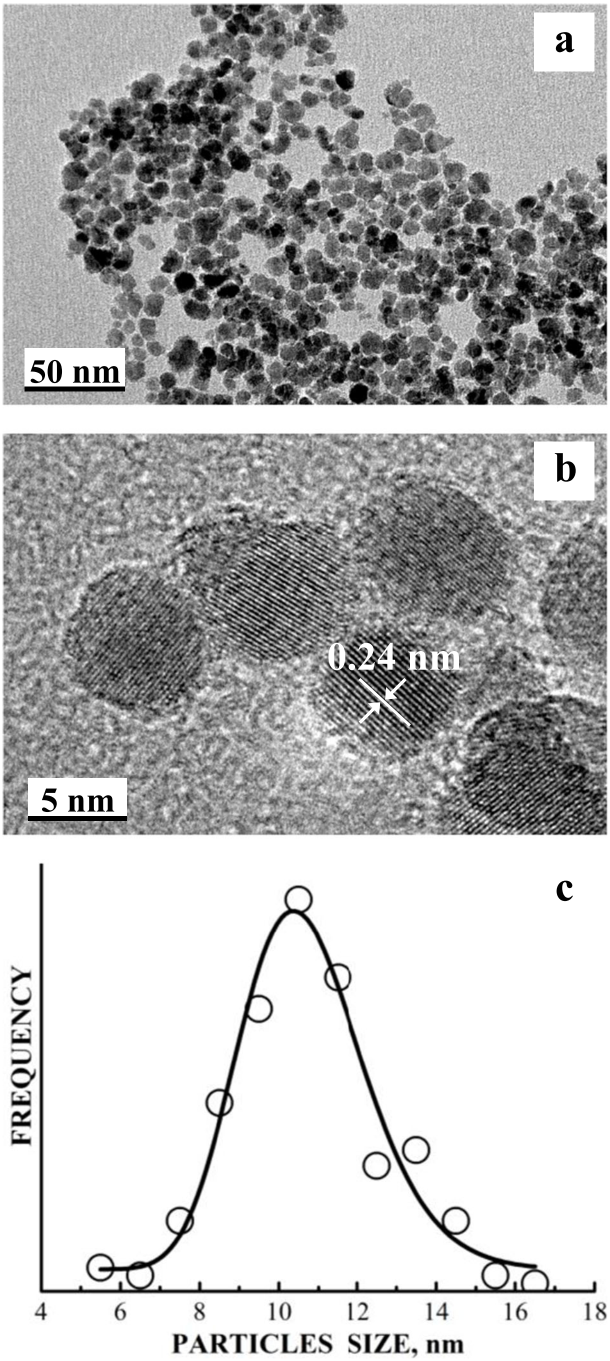

Fig. 3 Transmission and high resolution transmission electron microscopy images of as-prepared FM sample (**a** and **b**, respectively) and its particles' size distribution (**c**)

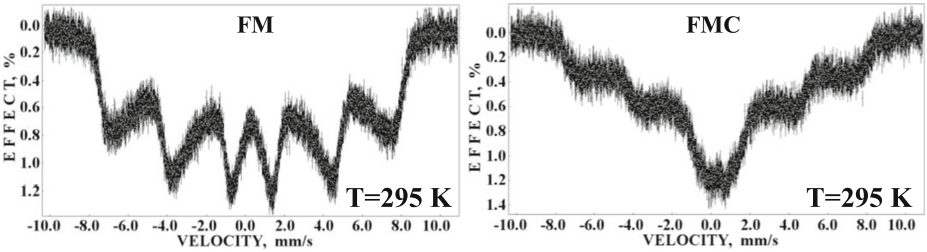

Fig. 4 The difference between the room temperature Mössbauer spectra of as-prepared FM and FMC nanoparticles

3 Results and discussion

The XRD pattern of the MF sample is shown in Fig. 2, being the recorded diffractogram typical of the maghemite/magnetite phase. Using the Scherrer's formula [16] for the broadening of the (311) XRD line, the average crystalline size of the MF sample is estimated to be ~9.3 nm.

Although there is a limitation of the XRD technique in magnetite and maghemite differentiation and in determination of the possible presence of both phases in the studied sample, the XRD peak positions in Fig. 2 indicate the predominance of maghemite phase in FM sample. Actually, apart for few extra peaks, such as (210) and (211) solely observed in pure maghemite (not seen in Fig. 2), XRD peaks of magnetite and maghemite are very analogous. However, the equivalent XRD peaks are slightly shifted towards the higher angles indicates the

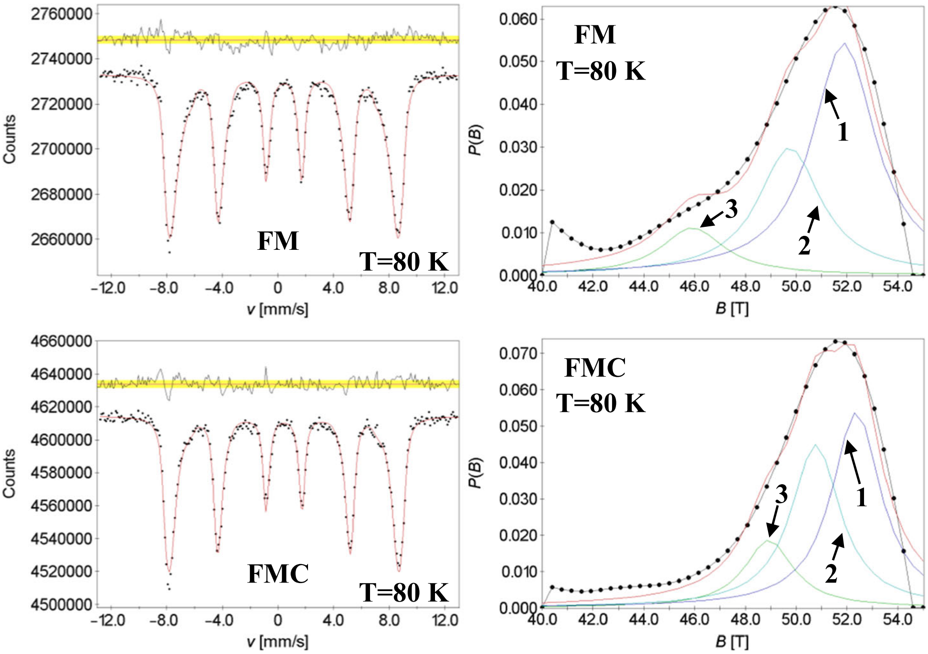

Fig. 5 Mössbauer spectra of as-prepared FM nanoparticles and those functionalized with citrate FMC nanoparticles measured at T = 80 K and fitted with hyperfine field distribution function, the differential spectra are shown on the top (left panel) and corresponding distribution functions of the hyperfine field (right panel). 1, 2 and 3 are Lorentzian single lines used for the fit of P(B)

Table 1 Parameters resulting from the fits of the hyperfine field distribution with three singlet Lorentzian lines for the FM and FMC Mössbauer spectra shown in Fig. 5

Sample	Singlet No	B_{max}, T	A, %
FM	1	51.9	57.1
	2	49.7	31.3
	3	45.9	11.6
FMC	1	52.4	45.9
	2	50.8	38.3
	3	48.9	15.8

predominance of maghemite phase. Particularly, quantitative shift of the (511) XRD peak towards 57.5° indicates complete conversion of magnetite into maghemite [17]. Moreover, the classical chemistry titration using $K_2Cr_2O_7$ (dichromatometry) was employed to determine the Fe^{2+} and Fe^{3+} contents in the FM and FMC samples. The Fe^{3+}/Fe^{2+} molar ratio was found to be about 2 after the first step of synthesis (fabrication of magnetite in Fig. 1). However, after oxidation of magnetite into maghemite NPs (step 2 of the synthesis), Fe^{2+} was not detected in the FM and FMC samples, corroborating with the XRD results of complete conversion of Fe_3O_4 into γ-Fe_2O_3.

The TEM and HRTEM images of the as-prepared FM sample are shown in Fig. 3. The as-prepared NPs reveal spherical shape. The assessed interatomic layer distance of 0.24 nm (see middle panel of Fig. 3) corresponds to the (311) plane in the maghemite phase. The size distribution of the as-prepared NPs (see Fig. 3c) demonstrates the average nanoparticles' diameter $< D >$ of 10.6 nm. As usual, the average crystalline size obtained from the XRD data (~9.3 nm) is slightly smaller than the average nanoparticles' diameter determined from the TEM data (10.6 nm), suggesting the presence of a surface crystalline dead layer.

The room temperature Mössbauer spectra of as-prepared FM and those functionalized with citrate FMC nanoparticles are shown in Fig. 4. The difference between the two spectra is clearly seen. Both spectra demonstrate relaxation character with different relaxation rates. The shape of the room temperature Mössbauer spectrum of as-prepared FM nanoparticles with more pronounced magnetically split pattern could be interpreted as a result of interparticle interactions which leads to slowing down of the magnetic relaxation. The shape of the room temperature Mössbauer spectrum of functionalized with citrate FMC nanoparticles with possible presence of doublet and smaller contribution of magnetically split component(s)

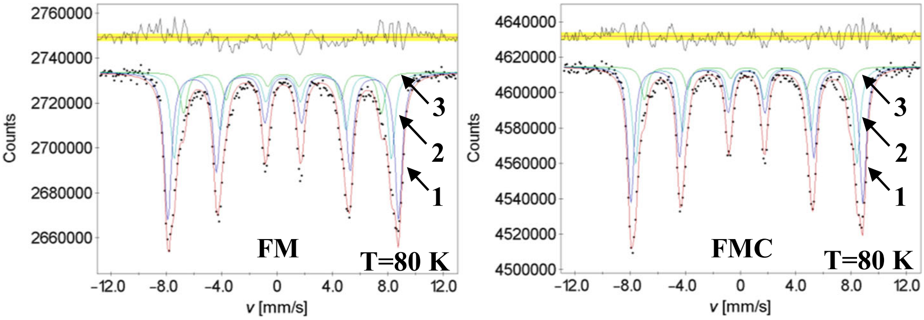

Fig. 6 Mössbauer spectra of as-prepared FM nanoparticles and those functionalized with citrate FMC nanoparticles measured at T = 80 K fitted with three independent sextets numbered 1, 2 and 3

Table 2 Mössbauer parameters for as-prepared FM nanoparticles and those functionalized with citrate FMC nanoparticles measured at T = 80 K

Γ, mm/s	δ, mm/s	2ε, mm/s	B_{hf}, T	A, %	Component
FM					
0.61 ± 0.04	0.45 ± 0.02	0.00 ± 0.02	51.8 ± 0.1	53.7	Sextet 1
0.61 ± 0.04	0.42 ± 0.02	−0.02 ± 0.02	48.8 ± 0.1	31.3	Sextet 2
0.61 ± 0.04	0.43 ± 0.02	−0.06 ± 0.02	44.4 ± 0.1	15.0	Sextet 3
FMC					
0.55 ± 0.04	0.45 ± 0.02	0.02 ± 0.02	52.2 ± 0.1	51.1	Sextet 1
0.55 ± 0.04	0.43 ± 0.02	−0.04 ± 0.02	49.8 ± 0.1	36.3	Sextet 2
0.55 ± 0.04	0.46 ± 0.02	−0.01 ± 0.02	46.1 ± 0.1	12.6	Sextet 3

can be explained as a result of (i) a decrease of interparticle interactions due to the NPs capping by citrate leading to the faster relaxation rate and (ii) the ^{57}Fe magnetic hyperfine field influenced by the electrostatic interaction of citrate polar molecules with iron oxide nanoparticles' surface leading to decrease of Fe spin disorder (see, for instance, [18]). Then the Mössbauer spectra of these samples were measured at 80 K.

The 80 K Mössbauer spectra of as-prepared FM nanoparticles and those functionalized with citrate FMC nanoparticles fitted with hyperfine field distribution function P(B) are shown in Fig. 5. Further the distribution functions were fitted using Lorentzian single lines and the best fit showed the presence of three single lines which can be related to three different ^{57}Fe microenvironments in nanoparticles. Parameters of these single component (single lines) in the distribution probabilities for FM and FMC samples are shown in Table 1. It is clearly seen small variations of B_{max} and A values for corresponding singlets for as-prepared FM nanoparticles and those functionalized with citrate FMC. This result indicates that the process of as-prepared FM nanoparticles interaction with citrate led to some changes in NPs after functionalization. Then to excavate more detailed Mössbauer parameters, these spectra were fitted using three independent sextets (Fig. 6). Mössbauer parameters for these sextets are collected in Table 2. The values of δ for all sextets are the same within the error while quadrupole shifts are almost the same. On the other hand, the values of B_{hf} for the same sextets in the Mössbauer spectra of FM and FMC nanoparticles are slightly different beyond the error. These values appeared to be slightly increased for sextets in the Mössbauer spectrum of nanoparticles functionalized with citrate FMC. This fact indicates that citrate capping of FM nanoparticles leads to small increase in the magnetic hyperfine field on the ^{57}Fe in corresponding microenvironments. Moreover, the relative areas for sextets 1 and 3 are slightly decreased while that for sextet 2 is slightly increased for the Mössbauer spectrum of FMC. This may indicate that functionalization of as-prepared FM nanoparticles with citrate caused re-distribution of the relative parts of three different ^{57}Fe microenvironments with increasing of the magnetic hyperfine fields on the ^{57}Fe.

4 Conclusion

The Mössbauer spectra of as-prepared iron oxide (maghemite) nanoparticles and those functionalized with citrate demonstrated different shapes at room temperature, indicating that the citrate capping of the NPs' surface may decrease the interparticle interaction while adding interaction of the polar end of the citrate molecules with the Fe^{3+} ions at the NPs' surface. Comparison of as-prepared IONs (sample FM) with the citrate functionalized NPs (sample

FMC) using 80 K Mössbauer spectroscopy demonstrated that the NPs can be considered as consisting of three slightly different ^{57}Fe microenvironments, with different magnetic hyperfine field values. The citrate functionalized NPs' lead to some re-distribution of the relative parts of these ^{57}Fe microenvironments, slighting increasing the corresponding magnetic hyperfine field. Neglecting the relaxation effects of potentially occurring particle size changes and leaving out redox reactions of nanoparticles by citric acid [10], our finding can be a result of the interaction of the polar end of the citrate molecules (carboxylate groups) with surface-terminating Fe^{3+}, leading to improvement of the surface spin ordering. This polar carboxylate-Fe^{3+} interaction can affect the magnetic properties of the surface of functionalized NPs.

Acknowledgements The authors thank LabMic-UFG for TEM measurements. M.H.S. and P.C.M. gratefully acknowledge financial support from Brazilian Agencies: Conselho Nacional de Desenvolvimento Científico e Tecnológico (CNPq) and Fundação de Apoio à Pesquisa do Distrito Federal (FAPDF). M.I.O., M.V.U. and V.A.S. were supported by the Ministry of Science and Higher Education of the Russian Federation and Act 211 of the Government of the Russian Federation, contract № 02.A03.21.0006. E.K. was supported by NKFIH-OTKA (the grant № 131963). This work was carried out within the Agreement of Cooperation between the Ural Federal University (Ekaterinburg) and the Eötvös Loránd University (Budapest).

References

1. Massart, R.: Preparation of aqueous magnetic liquids in alkaline and acid media. IEEE Trans. Magn. **17**, 1247–1248 (1981)
2. Goetze, T., Gansau, C., Buske, N., Roeder, M., Gornet, P., Bahr, M.: Biocompatible core/shell nanoparticles. J. Magn. Magn. Mater. **252**, 399–402 (2002)
3. Tombácz, E., Turcu, R., Socoliuc, V., Vékás, L.: Magnetic iron oxide nanoparticles: recent trends in design and synthesis of magnetoresponsive nanosystems. Biochem. Biophys. Res. Commun. **468**, 442–453 (2015)
4. Laurent, S., Forge, D., Port, M., Roch, A., Robic, C., Elst, L.V., Muller, R.N.: Magnetic iron oxide nanoparticles: synthesis, stabilization, vectorization, physicochemical characterization, and biological applications. Chem. Rev. **108**, 2064–2110 (2008)
5. Coelho, B.C.P., Siqueira, E.R., Ombredane, A.S., Joanitti, G.A., Chaves, S.B., da Silva, S.W., Chaker, J.A., Longo, J.P.F., Azevedo, R.B., Morais, P.C., Sousa, M.H.: Maghemite–gold core–shell nanostructures (γ-Fe_2O_3@Au) surface-functionalized with aluminium phthalocyanine for multi-task imaging and therapy. RSC Adv. **7**, 11223–11232 (2017)
6. Daou, T.J., Grenèche, J.M., Pourroy, G., Buathong, S., Derory, A., Ulhaq-Bouillet, C., Donnio, B., Guillon, D., Begin-Colin, S.: Coupling agent effect on magnetic properties of functionalized magnetite-based nanoparticles. Chem. Mater. **20**, 5869–5875 (2008)
7. Palma, S.I.C.J., Marciello, M., Carvalho, A., Veintemillas-Verdaguer, S., del Puerto Morales, M., Roque Ana, C.A.: Effects of phase transfer ligands on monodisperse iron oxide magnetic nanoparticles. J. Colloid Interface Sci. **437**, 147–155 (2015)
8. Cheraghipour, E., Javadpour, S., Mehdizadeh, A.R.: Citrate capped superparamagnetic iron oxide nanoparticles used for hyperthermia therapy. J. Biomed. Sci. Eng. **5**, 715–719 (2012)
9. Li, L., Mak, K.Y., Leung, C.W., Chan, K.Y., Chan, W.K., Zhong, W., Pong, P.W.T.: Effect of synthesis conditions on the properties of citric-acid coated iron oxide nanoparticles. Microelectr. Engin. **110**, 329–334 (2013)
10. da Silva, S.W., Guilherme, L.R., de Oliveira, A.C., Garg, V.K., Rodrigues, P.A.M., Coaquira, J.A.H., da Silva Ferreira, Q., de Melo, G.H.F., Lengyel, A., Szalay, R., Homonnay, Z., Klencsár, Z., Tolnai, G., Kuzmann, E.: Mössbauer and Raman spectroscopic study of oxidation and reduction of iron oxide nanoparticles promoted by various carboxylic acid layers. J. Radioanal. Nucl. Chem. **312**, 111–119 (2017)
11. Lengyel, A., Tolnai, G., Klencsár, Z., Garg, V.K., de Oliveira, A.C., Singh, L.H., Homonnay, Z., Szalay, R., Németh, P., Szabolcs, B., Ristic, M., Music, S., Kuzmann, E.: The effect of carboxylic acids on the oxidation of coated iron oxide nanoparticles. J. Nanopart. Res. **20**, 137 (2018)
12. Lengyel A., Garg V.K., de Oliveira A.C., da Silva S.W., Guilherme L.R., Klencsár Z., Homonnay Z., Coaquira J.A.H.,·Tolnai G., Kuzmann E. Mössbauer spectroscopy control of the preparation of citric- and mandelic acid functionalized nanomagnetites. Hyperfine Interact. **239**, 17 (2018)

13. Oshtrakh, M.I., Semionkin, V.A.: Mössbauer spectroscopy with a high velocity resolution: advances in biomedical, pharmaceutical, cosmochemical and nanotechnological research. Spectrochim. Acta, Part A: Mol. and Biomol. Spectroscopy. **100**, 78–87 (2013)
14. Oshtrakh M.I., Semionkin V.A.: Mössbauer Spectroscopy with a High Velocity Resolution: Principles and Applications. In: Proceedings of the International Conference “Mössbauer Spectroscopy in Materials Science 2016”, Eds. J. Tuček, M. Miglierini, AIP Conference Proceedings. AIP Publishing, Melville, New York, 2016, **1781**, 020019
15. Klencsár, Z., Kuzmann, E., Vértes, A.: User-friendly software for Mössbauer spectrum analysis. J. Radioanal. Nucl. Chem. **210**, 105–118 (1996)
16. Patterson, A.L.: The Scherrer formula for X-ray particle size determination. Phys. Rev. **56**, 978–982 (1939)
17. Kim, W., Suh, C.-Y., Cho, S.-W., Roh, K.-M., Kwon, H., Song, K., Shon, I.-J.: A new method for the identification and quantification of magnetite–maghemite mixture using conventional X-ray diffraction technique. Talanta. **94**, 348–352 (2012)
18. Oshtrakh, M.I., Ushakov, M.V., Šepelák, V., Semionkin, V.A., Morais, P.C.: Study of iron oxide nanoparticles using Mössbauer spectroscopy with a high velocity resolution. Spectrochim. Acta, Part A: Molec. and Biomolec. Spectroscopy. **152**, 666–679 (2016)

Affiliations

Michael V. Ushakov[1] • **M. H. Sousa**[2] • **Paulo C. Morais**[3,4] • **Ernő Kuzmann**[5] • **Vladimir A. Semionkin**[1] • **Michael I. Oshtrakh**[1]

[1] Institute of Physics and Technology, Ural Federal University, Ekaterinburg, Russian Federation 620002

[2] Green Nanotechnology Group, Faculty of Ceilândia, University of Brasília, Brasília, DF 72220-900, Brazil

[3] Catholic University of Brasília, Brasília, DF 70790-160, Brazil

[4] Institute of Physics, University of Brasília, Brasília, DF 70910-900, Brazil

[5] Laboratory of Nuclear Chemistry, Institute of Chemistry, Eötvös Loránd University, Budapest, Hungary